Research Paper

MULTIPLE SCLEROSIS JOURNAL | MSJ

Multiple Sclerosis Journal
19(7) 896–903

DOI: 10.1177/1352458512465135
msj.sagepub.com
SAGE

Increased iron accumulation occurs in the earliest stages of demyelinating disease: an ultra-high field susceptibility mapping study in Clinically Isolated Syndrome

Ali M Al-Radaideh[1,3], Samuel J Wharton[1], Su-Yin Lim[2], Christopher R Tench[2], Paul S Morgan[4], Richard W Bowtell[1], Cris S Constantinescu[2] and Penny A Gowland[1]

Abstract

Objective: To determine, using ultra-high field magnetic resonance imaging (MRI), whether changes in iron content occur in the earliest phases of demyelinating disease, by quantifying the magnetic susceptibility of deep grey matter structures in patients with Clinically Isolated Syndrome (CIS) that is suggestive of multiple sclerosis (MS), as compared with age-matched healthy subjects.

Methods: We compared 19 CIS patients to 20 age-matched, healthy controls. Scanning of the study subjects was performed on a 7T Philips Achieva system, using a 3-dimensional, T2*-weighted gradient echo acquisition. Phase data were first high-pass filtered, using a dipole fitting method, and then inverted to produce magnetic susceptibility maps. Region of interest (ROI) analysis was used to estimate magnetic susceptibility values for deep grey matter structures (caudate nucleus, putamen, globus pallidus, the thalamus and its pulvinar).

Results: Significantly increased relative susceptibilities were found in the CIS group, compared with controls, for the caudate nucleus ($p = < 0.01$), putamen ($p < 0.01$), globus pallidus ($p < 0.01$) and pulvinar ($p < 0.05$). We found no significant nor consistent trends in the relationship between susceptibility and age for either the study controls or CIS patients, in any ROI ($r^2 < 0.5$; $p > 0.05$). In CIS patients, the time elapsed since the clinical event and the Expanded Disability Status Scale (EDSS) scores were not correlated with iron levels in any ROI ($r^2 < 0.5$; $p > 0.05$); however, a moderate correlation ($r^2 = 0.3$; $p < 0.01$) was found between the T1 lesion load and the mean susceptibility of the caudate nucleus.

Conclusion: CIS patients showed an increased iron accumulation, as measured using susceptibility mapping of the deep grey matter, suggesting that iron changes did occur at the earlier stages of CIS disease.

Keywords

Deep grey matter, demyelinating disease, early MS, iron, magnetic resonance imaging, Clinically Isolated Syndrome, susceptibility mapping, ultra-high field, brain regions

Date received 8th June 2012; accepted 16th September 2012

Introduction

There is growing evidence of iron accumulation in the deep grey matter of patients with multiple sclerosis (MS), from both in vivo magnetic resonance imaging (MRI) and histopathological studies,[1] but it is not clear how early in the disease these changes occur. Our study addresses this question by taking advantage of the unique ability of ultra-high field (7T) MRI to detect iron deposition in the CNS, to assess iron concentration in the deep grey matter of patients

[1]Sir Peter Mansfield Magnetic Resonance Centre, University of Nottingham, UK.
[2]Clinical Neurology, University of Nottingham, UK.
[3]Medical Imaging Department, Hashemite University, Zarqa, Jordan.
[4]Medical Physics, Nottingham University Hospitals, UK.

Corresponding author:
Penny Gowland, Sir Peter Mansfield Magnetic Resonance Centre, School of Physics and Astronomy, University of Nottingham, NG7 2RD, UK.
Email: Penny.Gowland@nottingham.ac.uk

Table 1. Characteristics of study controls and the subjects with CIS.

Subjects	Controls	CIS patients	
N	20	19	
Sex (F/M)	7/13	10/9	
Mean age ± SD (years)	34.6 ± 9.4	36.63 ± 8.9	
Age range(years)	21–58	22–53	
Mean EDSS score ± SD		1.74 ± 0.9	
EDSS range		0–3.5	
Mean disease duration ± SD (years)		1.45 ± 1.22	
Disease duration range (years)		0.42–4.67	
Mean susceptibility ± SD			***p-value***
Caudate nucleus (ppm)	0.085 ± 0.016	0.102 ± 0.02	$p < 0.01$
Putamen (ppm)	0.081 ± 0.016	0.096 ± 0.015	$p < 0.05$
Globus pallidus (ppm)	0.118 ± 0.024	0.136 ± 0.024	$p < 0.01$
Thalamus (ppm)	0.053 ± 0.009	0.053 ± 0.008	
Pulvinar (ppm)	0.077 ± 0.013	0.090 ± 0.017	

CIS: Clinically Isolated Syndrome; EDSS: Expanded Disability Status Scale; F: female; M: male; N: number of subjects; ppm: parts per million

having Clinically Isolated Syndrome (CIS) that is suggestive of MS.

Many magnetic resonance (MR) parameters are sensitive to iron deposition, in particular T2 and T2*,[2–7] but T2 and T2* are also affected by other factors that are altered in MS, including myelination and inflammation. A recent study by Antonia et al.[8] compared the iron deposition in deep grey matter structures in CIS patients and age-matched healthy subjects, using a T2 hypointensity technique at 1.5T; and concluding that T2 hypointensity is found in CIS patients when compared to age-matched healthy controls, but that it was limited to the head of the caudate nucleus.

The change in magnetic susceptibility of a tissue due to iron accumulation causes field shifts that can be detected on phase images, which are more directly related to iron concentration than the relaxation times. Susceptibility-Weighted Imaging (SWI) combines T2* and phase information, increasing the sensitivity to iron;[9,10] however, phase and susceptibility-weighted images are both distorted by a non-local relationship between the underlying susceptibility distribution and the resulting field perturbation, which gives rise to the phase shifts.[11–13] Recently, quantitative susceptibility mapping techniques were developed that correct for this non-local relationship.[11–16] The field shifts due to magnetic susceptibility perturbations scale with field strength, making high-field imaging particularly sensitive for susceptibility mapping.

The aim of this study was to determine whether changes in iron content could be detected in the earliest phases of demyelinating disease, by employing ultra-high field MRI to quantify the magnetic susceptibility of deep grey matter structures in patients with CIS suggestive of MS, as compared to age-matched healthy subjects.

Materials and methods

Subjects

We recruited 20 patients with CIS (11 females, 9 males; mean age 36.6 years; age range 22–53) from Nottingham University Hospital, along with 20 age-matched healthy controls (7 females, 13 males; mean age 34.6 years; age range 21–58). One of the CIS patients' images showed significant motion artifact, so they could not be used in this study. Both groups gave informed consent. Table 1 summarises the characteristics of the two study groups. Neurological examinations were carried out by a doctor who was qualified to perform the Expanded Disability Status Scale (EDSS) assessments[17] according to the standardised scoring system in Neurostatus (http://www.neurostatus.net/scoring/index.php).

The patients were recruited prospectively, following their presentation with a CIS suggestive of MS, with symptoms not attributable to any other condition. One presented predominantly with spinal cord syndrome, eight with optic neuritis, three with an isolated brainstem syndrome and the rest with mixed central nervous system symptoms. Less than 1 month prior to the date of their scan, no patients received steroids nor were treated with disease-modifying therapy. Imaging was performed at a median of 11 months from the time of presentation (range, 7–56 months). Study subjects' conversion to clinically definite MS by the end of the first follow-up period was determined on the basis of clinical assessment, review of hospital notes and/or the presence of new demyelinating lesions upon follow-up imaging.

Of the 13 CIS who converted to MS, eight patients demonstrated radiological conversion without reporting new clinical symptoms. Converted and non-converted patients shared a median EDSS of 1.5 at baseline, with the converted group having an EDSS range of 1.0–3.5 as compared with 0–2.0 in the non-converted group, a difference that

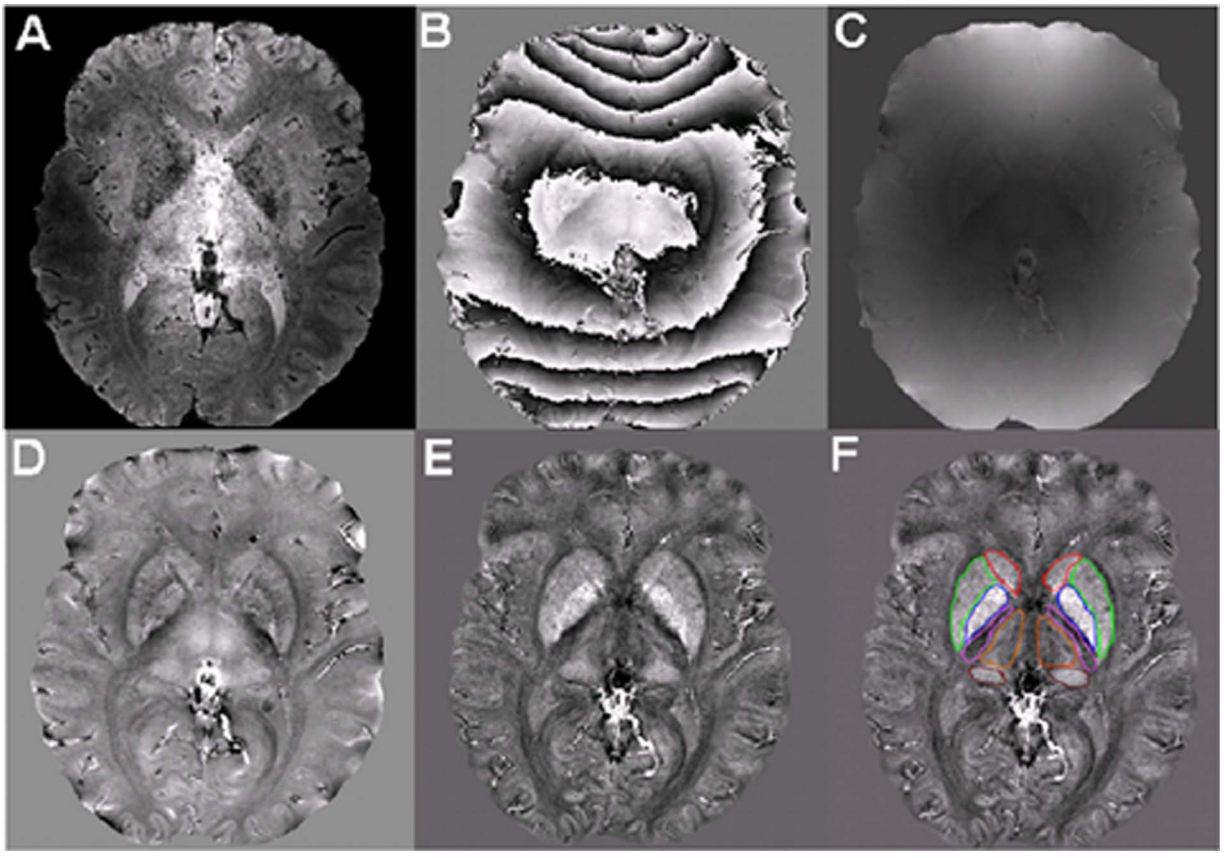

Figure 1. Output of this study's image-processing steps. (a) Magnitude data; (b) phase data; (c) unwrapped phase image; (d) unwrapped, filtered phase image; (e) susceptibility map; and (f) susceptibility map with all the ROIs drawn on it (red: caudate nucleus; green: putamen; blue: globus pallidus; purple: internal capsule; orange: thalamus and dark red: pulvinar).

was not statistically significant. The average age of patients who converted was slightly higher than the non-converted (38.9 years vs 31.2 years); however, this difference was also not statistically significant.

The subjects formed part of a longitudinal study of deep grey matter changes in CIS. We wanted to determine whether iron changes in their deep grey matter structures, in images obtained at baseline, would predict the likelihood of clinical or radiological conversion to MS between the baseline and the 1-year follow-up. Our study was approved by the Nottingham Research Ethics Committee and the University of Nottingham Research Ethics Committee (for patients and healthy controls, respectively).

MRI data acquisition

MRI scanning was performed on a 7T Philips Achieva system, equipped with a 16-channel receiving coil and a head-only volume transmitting coil. A 3-dimensional, T2*-weighted gradient echo sequence was acquired with the following settings: TR = 150 ms, TE = 20 ms, flip angle = 14°, SENSitivity Encoding (SENSE) factor = 2, Echo Planar Imaging (EPI) factor = 3, number of excitations = 1 and imaging time = 8.5 minutes. We acquired 200 transverse slices parallel to the Anterior Commissure -Posterior Commissure (AC-PC) line, in four interleaved stacks (with 5 mm overlap between each adjacent stack), to achieve a whole-head coverage with a relatively long TR. The spatial coverage was 192 × 164 × 25 mm per stack, with 0.5 mm isotropic voxel size.

Data processing and image analysis

For each subject, the four stacks of T2* weighted magnitude (Figure 1(a)) and its corresponding phase (Figure 1(b)), images were merged into a single volume. From the magnitude data, a binary mask of the brain was produced in FSL (www.fmrib.ox.ac.uk/fsl/) and this was applied to the phase data.[18] Prelude in FMRIB Software Library (FSL) was used to unwrap the resulting phase images within the mask (Figure 1(c)). These phase data were then high-pass filtered (Figure 1(d)) to remove the effects of large-scale background fields, for instance, near the air/tissue boundaries at the sinuses. This was achieved using a dipole fitting method.[11]

After filtering, the phase data were divided by $\gamma B_0 TE$ to yield field-shift maps. Susceptibility maps (Figure 1(e)) were then created from these filtered field maps, using a threshold-based method.[11] The relationship between the field and susceptibility distribution is local in the Fourier domain and it is given by the Equation (1), below:

$$\Delta\tilde{B}_z(\mathbf{k}) = B_0\tilde{\chi}(\mathbf{k})\left(\frac{1}{3} - \cos^2\beta\right) = B_0\tilde{\chi}(\mathbf{k})\cdot C(\mathbf{k}) \quad (1)$$

Here, the overstrike symbol ~ denotes a 3-dimensional Fourier transform, β is the angle between the k-vector and the k_z-axis, and C(k) represents the Fourier transformation of the dipole convolution kernel (in brackets in Equation 1, above) that link susceptibility and field. Rearranging this expression gave Equation (2):

$$\tilde{\chi}(\mathbf{k}) = \frac{\Delta\tilde{B}_z(\mathbf{k})}{B_0}\cdot\frac{1}{C(\mathbf{k})} \quad (2)$$

At $\beta = 54.7^o$ that is corresponding to a conical surface in k-space, C(k) tends to zero, and a 'division by zero' problem arises. This means that any noise in the field map close to this surface is amplified. A threshold, α, can be introduced such that any pixel with an associated $1/C(k) > \alpha$ is set to zero. This is equivalent to applying a conical mask in k-space to the 'badly behaved' k-space region, as defined by the threshold. The choice of α is important, as a large value will remove too much k-space and yield a susceptibility map with low contrast, while a small value for α will yield a susceptibility map dominated by noise artefacts.[11]

A small preliminary qualitative study on a single subject was carried out to determine the optimum threshold value. Through trial and error, a threshold value of $\alpha = 0.13$ was found to give a good compromise between noise and contrast. The use of a threshold will lead to an underestimation of susceptibility differences;[11] however, this underestimation is expected to be consistent between subjects, and as such, should not significantly alter the measured differences between control and patient groups. Merging of the stacks, high-pass filtering and the calculation of susceptibility maps were all done using Matlab (www.mathworks.com).

ROIs covering the caudate nucleus, putamen, globus pallidus, internal capsule, pulvinar of the thalamus, and the remaining thalamus (Figure 1(f)) were defined directly on the susceptibility maps in both hemispheres, on five slices that were completely encompassed by each region for all subjects, were performed manually (using MRIcro software; www.cabiatl.com/mricro/) by a trained radiographer who was blinded to their clinical symptoms. The susceptibility values for the different slices were averaged. Because only relative susceptibility can be measured, we calculated the difference in susceptibility of each structure relative to the internal capsule. The internal capsule was used as a reference, because it is a white-matter structure that is located very close to all other deep grey matter structures that were being studied and it is not a site with a known tendency to deposit iron when in a pathological state.[19] Also, the average phase in the same ROIs was calculated from the filtered phase map, and then this map was used to compare both the phase and susceptibility data.

Statistical analysis

A normality test was performed using the Kolmogorov-Smirnov test in Prism (GraphPad Software, US): The phase and susceptibility data showed a normal distribution. A two-way analysis of variance (ANOVA) was performed, to investigate the effects of regional and patient/control status (Prism, GraphPad Software, US) and then post hoc *t*-tests with False Discovery Rate (FDR) correction[20] were performed to investigate the effect of the patient/control status for each region, independently. The relationships between the susceptibility values of deep grey matter structures and the subject's age, EDSS score, disease duration, and T1 lesion load were examined using the Pearson correlation; however, the T2-weighted FLuid Attenuated inversion Recovery (FLAIR) sequence at 7T was still not optimized, so the T2 lesion load could not be calculated.

Results

Figure 2 demonstrates the non-local relationship between the underlying susceptibility distribution and the phase map, and its correction by susceptibility mapping. Figure 2(a) shows the magnitude image for orientation. In the phase map in Figure 2(b), it was seen that the iron-rich globus pallidus perturbed the magnetic field both locally (slightly positive offset within the borders of the globus pallidus region) and non-locally (negative phase offsets outside the globus pallidus). Figure 2(c) shows that susceptibility maps, produced by inversion of the phase images, provided better localized markers of iron content.

Figure 3 shows the susceptibility values in each ROI, relative to the susceptibility of the IC for the two groups. The two-way ANOVA showed that there was a significant difference between brain regions ($p < 0.0001$) and between patients and controls ($p < 0.0025$), and that there was a significant interaction between these factors ($p = 0.02$). A post-hoc *t*-test with Bonferroni correction showed that there was a significant difference between the two groups for the caudate nucleus ($p < 0.01$), putamen ($p < 0.01$) globus pallidus ($p < 0.01$) and pulvinar ($p < 0.05$).

There was a trend for the patients who later converted clinically or radiologically toward definite MS (13 patients), to having higher susceptibility values than those who did not (6 patients), but this difference was not found to be significant. When the non-converting CIS subjects were removed from the analysis, the statistical significance in the difference between controls and CIS (converting)

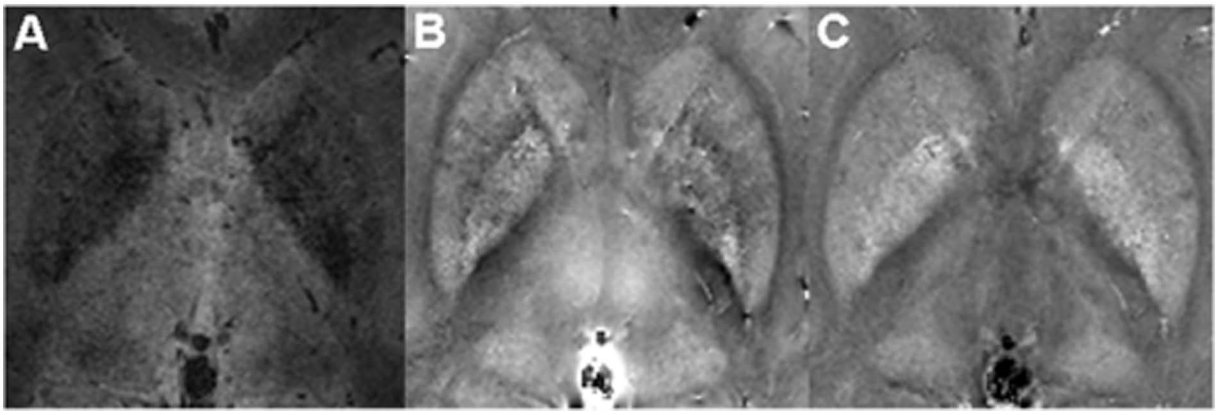

Figure 2. Appearance of deep grey matter structures on: (a) T*2 weighted image, (b) unwrapped-filtered phase image and (c) a susceptibility map.

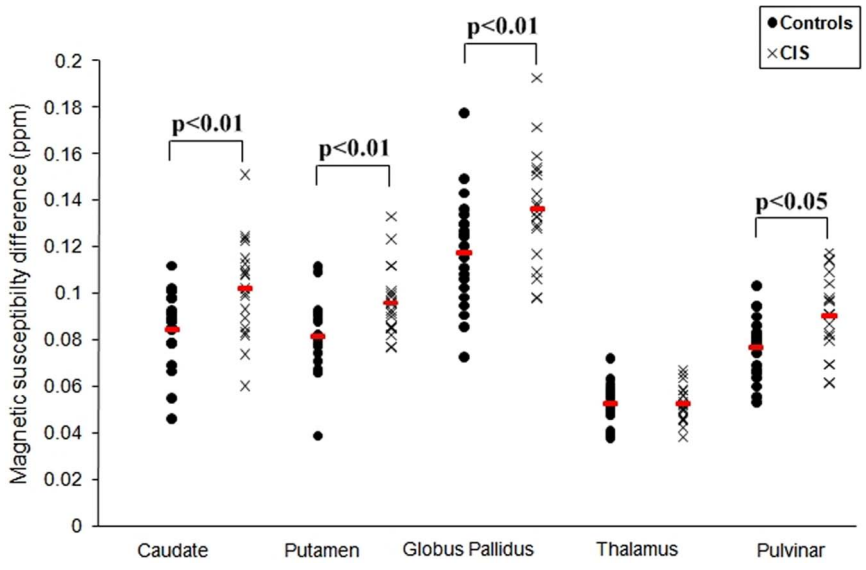

Figure 3. Differences in the magnetic susceptibility of various ROIs relative to the internal capsule, for all subjects in both study groups.

patients increased. In considering the phase data in Figure 4, a 2-way ANOVA showed significant differences between brain regions ($p < 0.0001$), but not between patients and controls ($p < 0.2$).

In order to test the consistency of drawing the ROIs, we drew the caudate nucleus, putamen, globus pallidus, thalamus and internal capsule regions five times and the coefficient of variation (CV) of the mean magnetic susceptibility revealed that the values were reproducible ($CV_{(caudate\ nucleus)}$ = 0.93 %; $CV_{(putamen)}$ = 0.67 %; $CV_{(globus\ pallidus)}$ = 1.47 %; $CV_{(thalamus)}$ = 0.47 % and $CV_{(internal\ capsule)}$ = 2.15 %, respectively).

No significant or consistent trends in the relationship between the susceptibility and age were found for either the controls nor CIS patients in any ROI ($r^2 < 0.5$; $p > 0.05$). In the CIS patients, the time elapsed since the clinical event was not correlated with iron levels in any ROI (r^2 <0.5; $p > 0.05$). Similarly, no significant association was detected between the EDSS scores and the susceptibility values in any region of interest in the CIS group; however, a moderate correlation ($r^2 = 0.3$; $p < 0.01$) was found between T1 lesion load and the mean susceptibility of the caudate nucleus.

Discussion

Deep grey matter structures, in particular the striatum and thalamus, play an important role in relaying motor, sensory, visual and cognitive information via extensive reciprocal connections with the cortex and other subcortical structures. They are susceptible to damage from inflammation arising in other areas. Thus, pathological changes in the deep grey matter may result in clinical disability. Deep grey

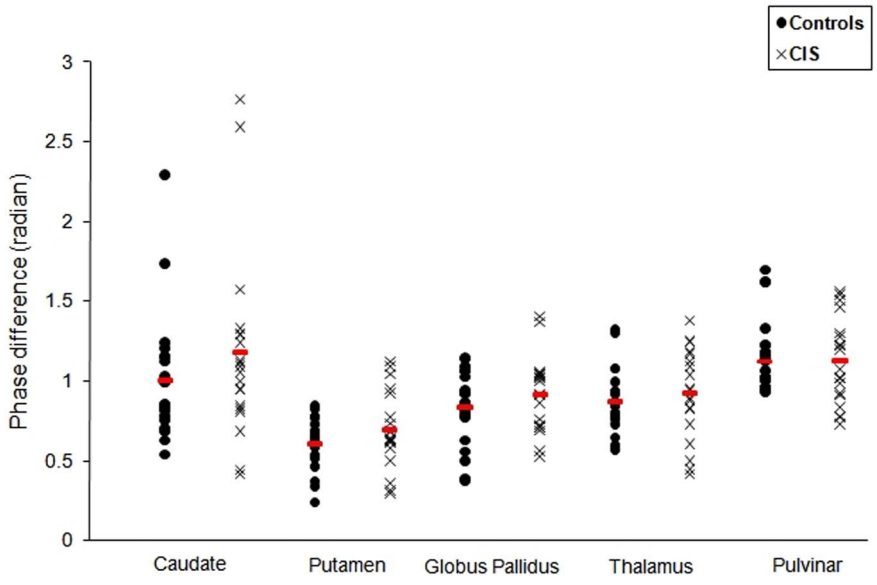

Figure 4. Difference of the phase of various ROIs relative to the internal capsule, for all subjects studied in the two groups.

matter involvement has been correlated with fatigue,[21,22] higher EDSS scores[23,24] and cognitive impairment[25] in MS patients.

This study is the first one to use quantitative magnetic susceptibility mapping to measure the iron accumulation in the deep grey matter structures in patients with CIS suggestive of MS.

In CIS patients, the deep grey matter areas studied had significantly-increased magnetic susceptibility, as assessed by MR susceptibility mapping, as compared to the healthy control subjects. This suggested that iron accumulation did occur in these regions, in the early phase of demyelinating disease. There was a trend for the change in iron content to be greater in the CIS patients who went on to convert to MS within a year, as compared to those who did not; however, this was not found to be statistically significant.

Our results suggested that different grey matter regions are affected to different extents by iron accumulation in CIS, although the relatively lower significance for the globus pallidus data may relate to the relatively low signal-to-noise ratio in that region, due to its short T2*. In other words, as the phase noise scales with the reciprocal of the image magnitude, a reduced signal due to the short T2* values in the globus pallidus is expected to lead to increased noise in the final susceptibility map.[15,16] Our study results suggested that different grey matter regions were affected to different extents by iron accumulation in CIS; although the relatively lower significance for the globus pallidus data may relate to increased phase noise, as a result of the particularly short T2* in this region, leading to a lower signal magnitude, thus propagating into the reconstructed susceptibility maps.[11]

Our study results support recent findings of significantly greater T2 hypointensity in the caudate nucleus of CIS patients, as compared to age-matched healthy controls.[26] A recent study by Hammond and colleagues uses phase data to show an increase in iron in the deep grey matter of definite MS patients, but it did not include any CIS patients.[27] In contrast, Khalil and colleagues[7] found that the R2* levels of basal ganglia are lower in patients with CIS than in healthy controls, concluding that iron deposition does not precede the development of MS disease, but may occur as a result of the disease itself.

The insignificant correlation found between susceptibility and the subject's age is not surprising, given the range of ages studied (21–58 years). Previous post-mortem[28] and in vivo data [10,29] suggest that iron accumulates rapidly from birth until about the end of the second decade, for nearly all brain regions, but tends to plateau in middle age. Two recent studies[2,7] report a correlation between R2* and age, but both report data for patient groups only, for whom iron accumulation may progress more rapidly, although one considered a wider age range (17–60 years)[2] and both used R2* as a measure of iron accumulation, which might be affected by other effects such as changes in water or myelin density.

The absence of any significant susceptibility changes in the thalamus can be attributed to the fact that the thalamus has a large amount of white matter between and within many grey matter nuclei, causing intrathalamic phase variation.[30]

In our study, susceptibility mapping was used to provide a method for overcoming the non-local relationship between field and phase images,[11,13,15,16] based on the development of a fast Fourier-based method for rapidly simulating the field shift caused by an arbitrary susceptibility distribution;[12,14] however, as susceptibility mapping increases sensitivity to noise, extra computational steps were required.

It should be noted that although tissue susceptibility is likely to be dominated by iron in these structures, the susceptibility of tissue depends on more than just the iron content. Recent work shows that myelin is diamagnetic relative to surrounding tissue, and also that this susceptibility offset is highly dependent on the underlying orientation of nerve fibers relative to the B_0.[31,32] Therefore, it is possible that the changes observed are due to or confounded by differences in myelination, as well as the changes in iron content. Finally, susceptibility values are relative, so the susceptibility of a region of the brain used for normalization must be assumed to be relatively stable, which could limit some applications of susceptibility mapping. In our studies, we measured susceptibility relative to the internal capsule, for the reasons stated above. This was based on the assumption that in the absence of visibly demyelinated lesions, the iron content of the internal capsule is likely to be more stable than that of the deep grey matter nuclei. Langkammer et al.[1] analysed iron content in various human brain structures, and indeed concluded that the frontal, temporal and occipital lobes' white matter had considerably lower iron content than the deep grey matter. In addition, the standard deviation was found to be significantly lower than that of deep grey matter structures. Although they did not analyse the internal capsule, it seemed likely to us that it would have a similar iron content to the rest of the white matter. In pathological situations that increase the iron content in deep grey matter, the internal capsule would likely be affected to a lesser degree.[19] Moreover, even if the internal capsule were to accumulate iron in the pathological processes of CIS/MS, the results expressed as differences were compared between CIS and healthy controls, so any increased iron content in the internal capsule in CIS would have only led to an underestimation of the differences between CIS and controls.

Besides iron effects, the internal capsule is known to have a high myelin content with highly ordered fiber directions.[33] As discussed above, myelin will affect the measured susceptibility. For this reason, small changes in the myelin content of the internal capsule between subjects would potentially reduce the sensitivity of the approach described here. This may explain why significant differences were not measured in the thalamic brain region.

In this work, high field (7T) was used to provide the necessary increase in signal-to-noise ratio; however, there are a number of potential problems using 7T. At 7T the T2* is reduced, but because of the relationship between susceptibility and phase scale as the product of field strength and echo time, shorter echo times can be used to overcome T2* signal attenuation at a high field. B1 inhomogeneity is another characteristic of 7T, but susceptibility maps are not affected by this. Furthermore, susceptibility maps are not limited by an increased power deposition, being based on gradient echo imaging sequences.[34]

The use of a threshold will underestimate susceptibility differences;[11] however, this underestimation is expected to be consistent between subjects and as such, should not significantly bias the differences between control and patient groups.

Our findings also provide further motivation for early anti-inflammatory and neuroprotective intervention in early MS/CIS, as it has the potential to prevent, delay, or mitigate later disease activity and progression.[35]

This study needs to be extended, in order to relate iron accumulation to the course of disease (e.g. conversion to MS, with prediction of disability) in CIS patients. Further studies will explore the relationship between deep grey matter iron accumulation and the likelihood of conversion to MS (or more generally, of a demyelinating relapse) within 1 year, as was suggested by the trend found in our study. The failure to reach significance may be explained by the relatively small number difference between the converters and non-converters. There is a need to further investigate the mechanisms linking iron deposition in areas unaffected by classical MS inflammatory demyelinating lesions, the presence of these lesions elsewhere in the CNS, quantitative changes in the white and grey matter and clinical disease activity. Our study indicated that there were subtle differences in grey matter susceptibility from the early phases of demyelination, but that there may be a window of opportunity for early treatment that could prevent more extensive damage and iron accumulation.

Funding

This work was supported by the UK Medical Research Council Programme Grant G0901321, and the Engineering and Physical Sciences Research Council. The 7T scanner was funded by the Welcome Trust and the Higher Education Funding Council of the UK. SYL was supported in part by an unrestricted educational grant from Teva Pharmaceuticals to CSC.

Conflict of interest

CSC has received research support, honoraria for tas, travel support for meetings and consultancy fees from Biogen Idec, Merck-Serono, Teva, Novartis, Bayer-Schering, GW Pharmaceuticals, and Morphosys.

References

1. Langkammer C, Krebs N, Goessler W, et al. Quantitative MR imaging of brain iron: A postmortem validation study. *Radiology* 2010; 257: 455–462.
2. Khalil M, Enzinger C, Langkammer C, et al. Quantitative assessment of brain iron by R2* relaxometry in patients with clinically isolated syndrome and relapsing–remitting multiple sclerosis. *Mult Scler* 2009; 15: 1048–1054.
3. Haacke EM, Cheng NYC, House MJ, et al. Imaging iron stores in the brain using magnetic resonance imaging. *Magn Reson Imaging* 2005; 23: 1–25.
4. Gelman N, Gorell JM, Barker PB, et al. MR imaging of human brain at 3.0 T: Preliminary report on transverse relaxation rates and relation to estimated iron content. *Radiology* 1999; 210: 759–767.

5. Graham JM, Paley MN, Grünewald RA, et al. Brain iron deposition in Parkinson's disease imaged using the PRIME magnetic resonance sequence. *Brain* 2000; 123: 2423–2431.
6. Ordidge RJ, Gorell JM, Deniau JC, et al. Assessment of relative brain iron concentrations using T2-weighted and T2*-weighted MRI at 3 Tesla. *Magn Reson Med* 1994; 32: 335–341.
7. Khalil M, Langkammer C and Ropele S. Determinants of brain iron in multiple sclerosis : A quantitative 3T MRI study. *Neurology* 2012; 77: 1691–1697.
8. Ceccarelli A, Rocca MA, Neema M, et al. Deep gray matter T2 hypointensity is present in patients with clinically isolated syndromes suggestive of multiple sclerosis. *Mult Scler* 2010; 16: 39–44.
9. Haacke EM, Makki M, Ge Y, et al. Characterizing iron deposition in multiple sclerosis lesions using susceptibility weighted imaging. *J Magn Reson Imaging* 2009; 29: 537–544.
10. Harder SL, Hopp KM, Ward H, et al. Mineralization of the deep gray matter with age: A retrospective review with susceptibility-weighted MR imaging. *Am J Neuroradiol* 2008; 29: 176–183.
11. Wharton S, Schäfer A and Bowtell R. Susceptibility mapping in the human brain using threshold-based k-space division. *Magn Reson Med* 2010; 63: 1292–1304.
12. Marques JP and Bowtell R. Application of a Fourier-based method for rapid calculation of field inhomogeneity due to spatial variation of magnetic susceptibility. *Magn Reson Engin* 2005; 25B: 65–78.
13. Shmueli K, De Zwart JA, Van Gelderen P, et al. Magnetic susceptibility mapping of brain tissue in vivo using MRI phase data. *Magn Reson Med* 2009; 62: 1510–1522.
14. Salomir P, Senneville BDD and Moonen CT. A fast calculation method for magnetic field inhomogeneity due to an arbitrary distribution of bulk susceptibility. *Magn Reson Engin* 2003; 19B: 26–34.
15. Liu T, Spincemaille P, De Rochefort L, et al. Calculation of susceptibility through multiple orientation sampling (COSMOS): A method for conditioning the inverse problem from measured magnetic field map to susceptibility source image in MRI. *Magn Reson Med* 2009; 61: 196–204.
16. De Rochefort L, Liu T, Kressler B, et al. Quantitative susceptibility map reconstruction from MR phase data using bayesian regularization: Validation and application to brain imaging. *Magn Reson Med* 2010; 63: 194–206.
17. Kurtzke JF. Rating neurologic impairment in multiple sclerosis - An Expanded Disability Status Scale (EDSS). *Neurology* 1983; 33: 1444–1452.
18. Smith SM. Fast robust automated brain extraction. *Hum Brain Mapp* 2002; 17: 143–155.
19. Onyszchuk G, LeVine SM, Brooks WM, et al. Post-acute pathological changes in the thalamus and internal capsule in aged mice following controlled cortical impact injury: A magnetic resonance imaging, iron histochemical, and glial immunohistochemical study. *Neurosci Lett* 2009; 452: 204–208.
20. Genovese CR, Lazar NA and Nichols T. Thresholding of statistical maps in functional neuroimaging using the false discovery rate. *Neuroimage* 2002; 15: 870–878.
21. Calabrese M, Rinaldi F, Grossi PS, et al. Basal ganglia and frontal/parietal cortical atrophy is associated with fatigue in relapsing–remitting multiple sclerosis. *Mult Scler* 2010; 16: 1220–1228.
22. Niepel G, Tench CR, Morgan PS, et al. Deep gray matter and fatigue in MS. A T1 relaxation time study. *J Neurol* 2006; 253: 896–902.
23. Tao G, Datta S, He R, et al. Deep gray matter atrophy in multiple sclerosis: A tensor based morphometry. *J Neurol Sci* 2009; 282: 39–46.
24. Davies GR, Altmann DR, Rashid W, et al. Emergence of thalamic magnetization transfer ratio abnormality in early relapsing–remitting multiple sclerosis. *Mult Scler* 2005; 11: 276–281.
25. Houtchens MK, Benedict RH, Killiany R, et al. Thalamic atrophy and cognition in multiple sclerosis. *Neurology* 2007; 18: 1213–1223.
26. Ceccarelli A, Rocca MA, Neema M, et al. Deep gray matter T2 hypointensity is present in patients with clinically isolated syndromes suggestive of multiple sclerosis. *Mult Scler* 2010; 16: 39–44.
27. Hammond KE, Metcalf M, Carvajal L, et al. Quantitative in vivo magnetic resonance imaging of multiple sclerosis at 7 Tesla with sensitivity to iron. *Ann Neurol* 2008; 64: 707–713.
28. Hallgren B and Sourander P. The effect of age on the non-haemin iron in the human brain. *J Neurochem* 1958; 3: 41–51.
29. Aquino D, Bizzi A, Grisoli M, et al. Age-related iron deposition in the basal ganglia: Quantitative analysis in healthy subjects. *Radiology* 2009; 252: 165–172.
30. Fujita N, Tanaka H, Takanashi M, et al. Lateral geniculate nucleus: Anatomic and functional identification by use of MR imaging. *Am J Neuroradiol* 2001; 22: 1719–1726.
31. Xiang HE and Yablonskiy DA. Biophysical mechanisms of phase contrast in gradient echo MRI. *PNAS* 2009; 13558–13563.
32. Lee J, Shmueli K, Fukunaga M, et al. Sensitivity of MRI resonance frequency to the orientation of brain tissue microstructure. *PNAS* 2010; 107: 5130–5135.
33. Wakana S, Jiang H, Nagae-Poetscher LM, et al. Fiber tract-based atlas of human white matter anatomy. *Radiology* 2004; 230: 77–87.
34. Deistung A, Rauscher A, Sedlacik J, et al. Susceptibility weighted imaging at ultra high magnetic field strengths: Theoretical considerations and experimental results. *Magn Reson Med* 2008; 60: 1155–1168.
35. Stankiewicz J, Panter SS, Neema M, et al. Iron in chronic brain disorders: Imaging and neurotherapeutic implications. *Neurotherapeutics* 2007; 4: 371–386.